Materials and Design 31 (2010) 2078–2084

Contents lists available at ScienceDirect

Materials and Design

journal homepage: www.elsevier.com/locate/matdes

Single and double-step stress relaxation and constitutive modeling of viscoelastic behavior of swelled and un-swelled natural rubber loaded with carbon black

M. Abu-Abdeen *

Physics Department, College of Science, King Faisal University, Al-Hasa, 31982, P.O. Box 400, Saudi Arabia

ARTICLE INFO

Article history:
Received 19 August 2009
Accepted 2 October 2009
Available online 8 October 2009

Keywords:
Stress relaxation
Viscoelasticity
Swelling
Natural rubber

ABSTRACT

A phenomenological one-dimensional constitutive model, characterizing the mechanical behavior of viscoelastic natural rubber filled with the percolation concentration of HAF carbon black is developed in this investigation. This simple differential form model is based on a combination of linear and non-linear springs with dashpots, incorporating typical polymeric behavior such as shear thinning, thermal softening and non-linear dependence on deformation. The material parameters for this model are determined for the investigated vulcanizates. The model was also developed on same samples after immersion in kerosene for different intervals of times. One step mechanism of relaxation was appeared for straining the samples to different strain levels with constant strain rate. On the other hand, two step mechanisms of relaxation were appeared on straining specimens to same strain level but with different strain rates.

1. Introduction

Scientific and technological interest attaches to the understanding of viscoelastic behavior of polymers. To provide information about the viscoelastic properties of these materials, various experimental techniques have been used, among which the stress relaxation is one of the simplest. Previous studies on the effect of processing conditions, prior strains and strain rates [1–8] have been performed. The stress relaxation denotes the process of the establishment of static equilibrium in a physical or a physico-mechanical system. Its rate depends on the probability of the transition of the system from one stage of equilibrium to another [9]. The ideal crosslinked rubber behaves like a perfect Hookean spring. When it is under constant strain, the resulting stress remains constant as long as it is strained, and so it is time independent. When the strain removed, the stress returns to zero instantaneously, and the material recovers its original dimensions. Hence, no decrease in stress is observed during stress relaxation experiments of an ideal crosslinked rubber. However, when a real viscoelastic rubber is strained at a constant rate as rapidly as possible to attain a fixed deformation, the stress required to maintain that fixed strain is found to decay with time. Stress relaxation may be one-stage or two stage mechanism in multiphase systems [10]. Two-process model for stress relaxation is introduced [3,4]. It assumed that the stress relaxation in polymers can be represented by two thermally activated processes acting in parallel. The first one is a consequence of propagation of the defects through the material. The second one occurs in the amorphous fraction.

Three following processes can occur during stress relaxation of a typical rubber vulcanizate: (a) physical relaxation, which occurs due to relocation of the rubber chains and the fillers, when subjected to deformation. However, this happens within a very short span of time right after deformation in a rubber vulcanizate that is crosslinked well above its gel point (as observed in actual practice). Also it is due to the entropic removal of order; that is, the molecules return to the most stable conformation. This results in higher entropy. This happens because of weak secondary van der Waal's forces, which constitute the intermolecular interaction. The amorphous nature and greater mobility of flexible chains in rubbers is also a reason for the increase in entropy. Thus, a reorientation of the molecular network occurs with the disengagement and re-engagement of chain entanglements, which breaks the secondary bonds between chains, filler particles, and chain and filler particles [11]. As a result, internal relaxation occurs, and so the force (and stress) needed to sustain the constant strain decreases with time. Because the molecular reorganization is temperature dependent, the relaxation is more rapid at higher temperatures. (b) Degradation, this is caused by heat, light, oxygen/air, and chemicals, which result in decrosslinking and/or chain scission. All of these would possibly reduce the counter force during stress relaxation testing. (c) Crosslinking, breaking and subsequent

* Present address: Physics Department, Faculty of Science, Cairo University, Giza, Egypt. Tel.: +966 535800000x1885, mobile: +966 5551750385; fax: +966 535886437.
E-mail address: mmaabdeen@yahoo.com

0261-3069/$ - see front matter © 2009 Elsevier Ltd. All rights reserved.
doi:10.1016/j.matdes.2009.10.006

rearrangement of the crosslinks and/or polymer backbone as well as combination of oxygenated species (originated from degradation) can form additional crosslinks. However, this does not contribute to "normal" stress relaxation as the new crosslinks are formed in the load bearing condition [12–14].

In the present work modeling of the viscoelastic behavior of unswelled and swelled natural rubber vulcanizates are done. Stress relaxation at different strain levels with constant strain rate is also studied. The effect of different straining rate on the stress relaxation mechanisms is also studied.

2. Experimental

2.1. Materials

Commercial grades of natural rubber NR and used as polymer matrix. High abrasion furnace (HAF-N330, particle size diameter ranges from 28 to 36 nm, tensile strength 22.4 MPa) carbon black was used as reinforcement filler. Other compounding ingredients like zinc oxide and stearic acid (activators), dibenz thiazyl disulfide (MBTS, semiultra accelerator), phenylnaphthyl-amine (PBN, antioxidant, melting point 105 °C), and sulfur (vulcanizing agent) were used. All these materials were purchased from Alexandria trade rubber company (TRENCO, Alexandria, Egypt).

2.2. Compounding and curing

A master batch of NR loaded with 40 phr (parts per 100 parts of rubber by weight) of HAF carbon black was prepared. Samples were prepared according to the recipes presented in Table 1. The compounds were mixed according to the ASTM D 3182-07 method in a laboratory-sized mixing mill at a friction ratio of 1:1.19, by carefully controlling the temperature, nip gap, time of mixing, and uniform cutting operation. The temperature range for mixing was 60–70 °C. The order and time periods of mixing were as follows: 0–3 min mastication; 3–6 min addition of one-third filler plus one-third oil; 6–13 min addition of one-third filler and one-third oil; 13–18 min addition of remaining filler and oil; 18–26 min addition of other ingredients; 26–30 min refining through tight nip gap and dump (the nip gap was 1.5 mm). After mixing, the rubber compositions were molded in an electrically heated hydraulic press to the optimum cure using molding conditions that were previously determined from torque data using a Monsanto rheometer (R100) according to ASTM D5099-08. Samples were then aged according to ASTM D3182-07 method for 60 days at 70 °C.

2.3. Stress relaxation measurements

Samples were cut using a dumb-bell shape cutter and had dimensions as indicated in Fig. 1. Some of these samples were immersed in kerosene for different time intervals and swelled according to ASTM D3616-04 method. Stress relaxation measurements according to ASTM D1646-7 method for un-swelled and swelled samples after dried well were carried out at 25 °C using an Instron tensile machine type Instron 3345J8621.

Table 1
Mix formation of 40 HAF/NR composites.

	Ingredients							
	NR	HAF	Processing oil	Stearic acid	MBTS[a]	PBN[b]	Zinc oxide	Sulfur
phr	100	40	10	2	2	1	5	2

[a] Dibenthiazole disulphate.
[b] Phenyl-β-naphthylamine.

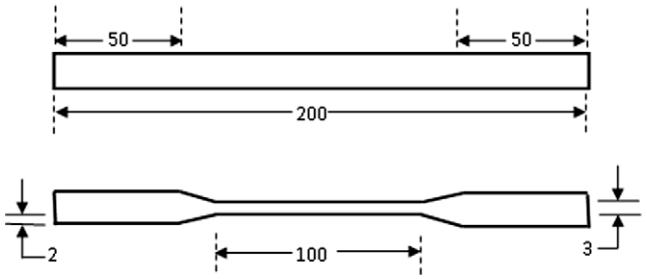

Fig. 1. Dimensions of specimen for stress-relaxation test (all dimensions are in millimeters).

3. Results and discussion

3.1. Step relaxation

A two-step relaxation mechanism has been reported in different articles for different materials [15–18]. Some of which adjusts to a single episode for pure rubber and a two stage processes for the reinforced materials.

Fig. 2 presents the relation between the stress and log(t) for the 40HAF/NR vulcanizate strained to different strain levels with a constant straining strain rate of 30 mm/min. The graph shows straight lines relations. Each line has one slope (one step relaxation) and differs from one line to another. This indicates one mechanism of relaxation takes place. The data in Fig. 2 is found to obey a straight line equation of the form (see Table 2):

$$\sigma(t) = \sigma_0 - k\ln(t) \quad (1)$$

where σ_0 is the initial stress subjected to the specimen at zero time and k represents the slope of the lines and its values are listed in Table 3.

Fig. 3 illustrates plots between the stress and log(t) of the studied rubber vulcanizates to a same final strain levels of 500% but at

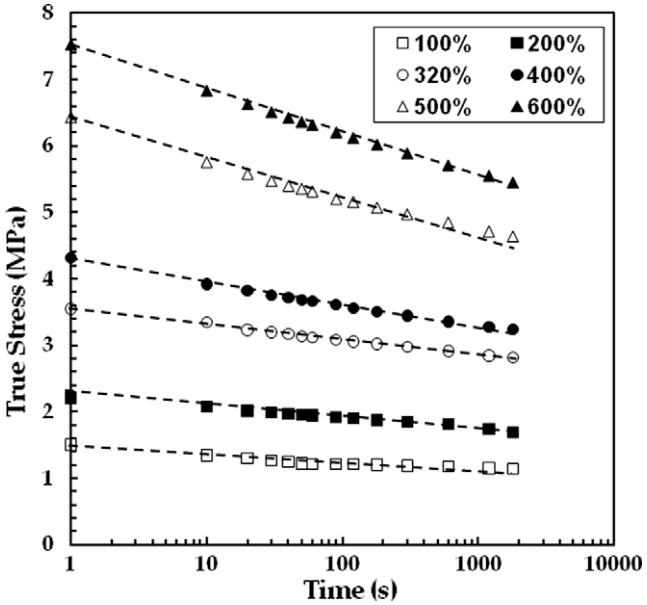

Fig. 2. A plot between stress and time (log scale) of 40HAF/NR at different strain levels at a strain rate of 30 mm/min (points = experimental data, dashed lines = theoretic calculations).

Table 2
The calculated values of t_s, slope 1, slope 2 and the intersection with the vertical axis at different strain rates and constant strain level of 500%.

Strain rate (mm/min)	t_s (s)	Slope1 (MPa)	Slope 2 (MPa)	Intersection (MPa s)
100	2.400	1.1	1.1	1220
200	2.410	1.12	0.89	1250
300	2.400	1.31	0.92	1185
400	2.415	1.20	0.88	1150
500	2.410	1.33	0.96	1210

Table 3
Material constants at different strain levels and constant strain rate of 30 mm/min.

Strain level (%)	$c_1 = E_1$ (MPa)	c_2 (MPa)	n_2	$E_2 = c_2\varepsilon^n$ (MPa)	η (MPa s)	τ (min)	k (MPa)
100	2.400	1.1	−0.35	1.1	1220	18.48	0.045
200	2.410	1.12	−0.35	0.89	1250	23.71	0.067
320	2.400	1.31	−0.30	0.92	1185	21.37	0.099
400	2.415	1.20	−0.27	0.88	1150	21.68	0.141
500	2.410	1.33	−0.20	0.96	1210	20.92	0.233
600	2.380	1.28	−0.17	0.94	1200	21.19	0.273

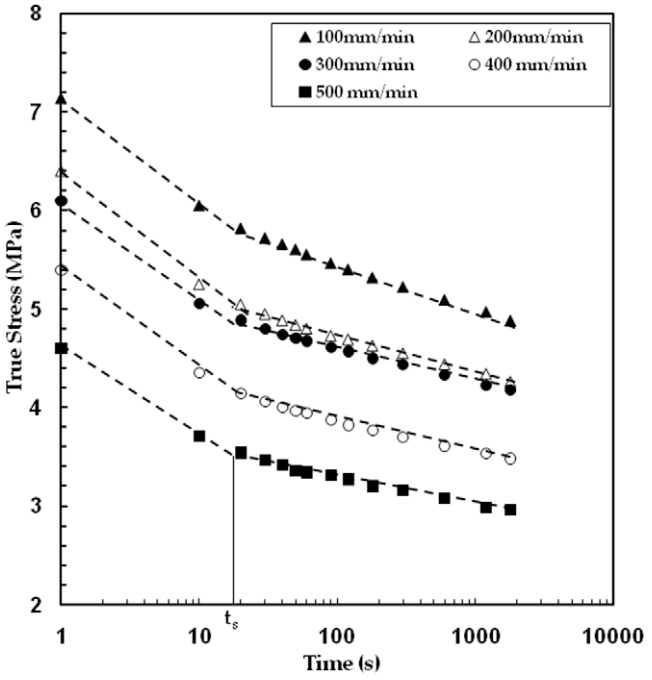

Fig. 3. A plot between stress and time (log scale) of 40HAF/NR at different strain rates and constant strain level of 500% (points = experimental data, dashed lines = theoretic calculations).

different strain rates. It is interesting to note that in all cases the points fall on two intersecting straight lines, unlike the behavior reported by same vulcanizate but strained at different strain levels at constant strain rate shown in Fig. 2. The stress relaxation plot consisting of two straight lines of unequal slopes indicates different mechanisms of relaxation. One mechanism operates at very short times (slope 1) and the other one is prominent at the later stage of relaxation (slope 2) [19]. Table 2 shows the features that characterize the two lines, slopes, intercepts and the point of intersection of these two straight lines denoted by t_s in the table that is the time at which a changeover takes place from one mechanism to the other. The slope at short times is steeper than the slope at long times indicating a faster stress relaxation and thus a faster process. An explanation, assuming that the short term part of the relaxation is associated with small segments or domains of molecular chains and/or the orientation at the filler–matrix interface. Whereas the long term part relaxation is caused by a long-range rearrangement of molecular chains and/or it is due to the progressive failure of polymer–filler bonding [17]. This was explained on the basis of soft and hard segments present in polymers, in which the hard segments act as physical crosslinks. The initial relaxation may be also due to the orientation at the interface of hard and soft segments and the second one is due to the flow of the soft matrix under tension at longer times [16].

3.2. Theoretic background

When a constant strain is applied to a rubber sample crosslinked well above its gel point, the force required for maintaining the strain decreases with time. This behavior is called "stress relaxation". Both physical and chemical processes can cause the stress relaxation depending upon the time scale. At ambient conditions and/or short times, the stress relaxation predominantly results from physical processes. At higher temperatures or in degradative environments, and/or for long time exposures, chemical processes dominate over physical processes [20].

Unvulcanized rubbers contain a large number of molecular chains of different lengths. Being viscoelastic material, rubbers exhibit characteristics of both viscous and elastic materials. Because of crosslinking, the viscous behavior of the rubber decreases, and the elasticity increases. In practice, crosslinked rubbers (unfilled) are imperfect network structures that contain chain ends, loops in rubber chains, branched molecules that are partly incorporated into the network, molecules entrapped in the network but not attached to it by chemical bonds, and so on. Hence, when the strain is removed, the stress does not return to zero, and so the material does not recover its original dimensions. Therefore, the stress relaxation curve levels off to a finite stress instead of zero stress at long times [21].

Thus, the freedom of movement of rubber chains depends on the degree of crosslinking, crystallinity, molecular dimensions, perfection, morphology of the network structure and environmental conditions. Hence, the rate of stress relaxation of a rubber molecule depends on its surrounding structure and will be different from other molecules even in a homogeneous, unfilled rubber compound.

The classical linear theory of viscoelasticity can basically be presented by two major forms: hereditary integrals or differential forms. Even though the differential constitutive forms are not as general [22] as the hereditary integral representations, they are more commonly used. This fact is mostly due to the more appealing usage of parameters such as stress/strain and stress/strain rates, as opposed to relaxation and creep kernels. Furthermore, the differential forms can be directly related to the intuitive spring and dashpot diagrams. It is recalled here that a linear spring constitutive equation is of the form $\sigma_s = E\varepsilon_s$, where σ_s and ε_s are the stress and the strain in the spring, respectively. E is the constant modulus of the spring and implies a linear elastic stress–strain relationship. Similarly, a linear dashpot constitutive equation is of the form $\sigma_d = \eta\varepsilon_d$, where σ_d and ε_d are the stress and strain rate in the dashpot, respectively. η is the constant viscosity and implies a Newtonian viscous effect.

We consider now a popular combination of springs and dashpot, the so-called standard solid model, shown by Fig. 4 and composed of a Maxwell element (linear spring and dashpot in series) with a linear spring in parallel. The stress in the standard solid is the sum of the stresses in the Maxwell element and the linear

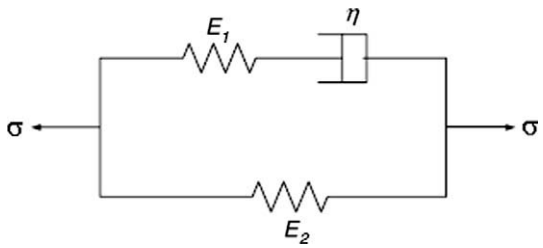

Fig. 4. Three-element standard solid model.

spring. The governing equation for the system can be readily derived as:

$$\frac{\eta}{E_1}\frac{d\sigma}{dt}+\sigma=\frac{\eta}{E_1}(E_1+E_2)\frac{d\varepsilon}{dt}+E_2\varepsilon \tag{2}$$

where η, E_1 and E_2 are material constants, σ and ε are the stress and strain respectively.

More generally, any linear viscoelastic differential model can be expressed as follows [23]:

$$\left(p_0+p_1\frac{\partial}{\partial t}+p_2\frac{\partial^2}{\partial t^2}+\ldots\right)\sigma(t)=\left(q_0+q_1\frac{\partial}{\partial t}+q_2\frac{\partial^2}{\partial t^2}+\ldots\right)\varepsilon(t) \tag{3}$$

where p's and q's are material constants. The differential form of Eq. (3) solely involves current strain, stress, strain rates, stress rates and higher derivatives.

An important observation should be made regarding Eq. (3). The time dependent component of stress relaxation processes is described by a summation of exponential terms, namely

$$\sigma(t)=c_0+c_1e^{-t/\tau_1}+c_2e^{-t/\tau_2}+\ldots+c_ne^{-t/\tau_n} \tag{4}$$

where c's are constants and τ's are relaxation times. It has been noted that the time dependent component of the stress relaxation of polymers, say $g(t)$, very often follows a simple power law-type behavior $g(t) = t^n$ [22]. In order to Eq. (4) to adequately approximate this feature, many exponential terms may be required.

Many non-linear theories have been proposed [22]. Most of them follow a similar pattern. Analogous to the linear case, they are based on the axion that the stress in a viscoelastic material depends on the entire deformation history; or alternatively, the strain in a viscoelastic material depends on stress history.

A popular approach to model non-linear viscoelastic behavior has been the use of differential constitutive relations [24]. Various differential forms are based on springs and dashpots combinations. The analytical solution for single-step stress relaxation processes (i.e., $\varepsilon = \varepsilon_0 H(t)$; where $H(t)$ is the heaviside function) is determined from Eq. (2) yielding:

$$\sigma(t)=E_2\varepsilon_o+E_1\varepsilon_o\exp\left(-\frac{E_1t}{\eta}\right) \tag{5}$$

Fig. 5 shows the schematic of stress-relaxation exhibited by using the standard solid model. The trends of typical polymeric behavior are well captured by this simple model making it a good starting point for the development of an advanced model. However, in order to adapt and exploit the differential form of the standard solid model to characterize finite non-linear deformation of real polymers, various changes with regards to the definitions of stress, stress rate, strain and strain rate need to be introduced for finite deformation.

In the determination of the constitutive equation for the modified standard solid model, various springs and dashpots were utilized. Fig. 6 depicts the arrangement used for this study. It basically represents a Maxwell element connected in parallel with a Kelvin solid (except E_2 is not a linear spring). The spring E_1 is considered to be a material constant dependent only on operating

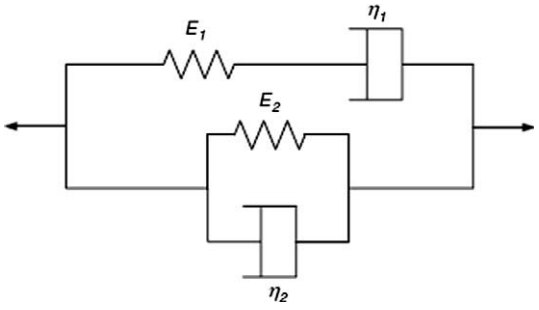

Fig. 6. Rheologic schematic of the modified standard solid model.

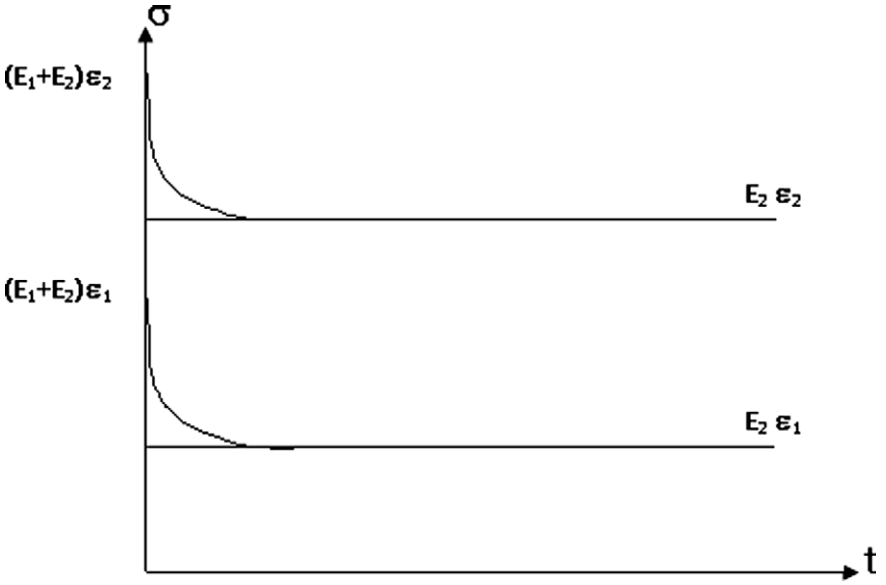

Fig. 5. Relaxation response of the standard solid model.

temperature, whereas the other spring, E_2, is assumed to be a non-linear spring dependent on the level of deformation as well as temperature. The equation for viscosity used for the two dashpots in the study was not taken to be a constant quantity, rather it was considered to be a function of strain rate and temperature. The form of the viscosity term, η, is given in by the form [25]:

$$\eta(\dot{\varepsilon},t)=\left\{\eta_\infty+\frac{\eta_o-\eta_\infty}{\left[1+(a|\dot{\varepsilon}|)^2-(\frac{|\dot{\varepsilon}|}{10^5})^d\right]^b}\right\}\left[\frac{T_r-T_{vf}}{T-T_{vf}}\right]^m \tag{6}$$

where η_0 is the viscosity at zero strain-rate and η_∞ is the asymptotic viscosity at $\dot{\varepsilon}=\infty$ with $\dot{\varepsilon}$ is the strain rate experienced by each dashpot (note that the strain rates in the two dashpots are not the same). The material parameters a, d and b serve to adjust the decay of shear thinning under increasing strain rate. The material parameter, m, adjusts the response of viscosity of the polymer with different temperatures. Here, T_{vf} is the Vogel–Fulcher temperature term [26], taken from the well-known Vogel–Fulcher–Tammann law [26], which relates viscosity as a function of temperature. T_{vf} is usually taken 50 K below the experimental glass transition temperature. T_r is the reference temperature or the room temperature in the present study. T is the temperature at which the experiment is performed.

The behavior of the two springs E_1 and E_2, for the standard solid model during stress relaxation, present a dependency on the strain, not on strain rate. Hence, it seems that the spring components of the modified standard solid model are composed of two distinct modes, the loading and the relaxation mode. Based on this idea, the springs E_1 and E_2 in the modified standard solid model are redefined in the following form:

$$E_1=c_1\left(1+\frac{T_r-T}{T_d}\right) \tag{7}$$

$$E_2=c_1\varepsilon^{n_2}\left(1+\frac{T_r-T}{T_d}\right) \tag{8}$$

Here, c_1, c_2 and n_2 are material parameters and ε is the true stain of the material. T_r, T_d and T are the room, the melting or decomposition (473 K) and the operating temperatures, respectively. It should be emphasized that many other forms of nonlinearities, i.e., rubber elasticity, might be implemented instead of the simple power law utilized in Eq. (8). However, this would lead to a more complex model and correspondingly more number of material parameters.

Fig. 6 shows the "rheologic" schematic of the modified standard solid model incorporating the new concepts discussed above. The constitutive equation of the developed constitutive model, for room temperature, may finally be expressed as:

$$\frac{c_1}{\eta_1}\sigma+\dot{\sigma}=c_1\dot{\varepsilon}+\frac{c_1}{\eta_1}c_2\varepsilon^{(n_2+1)}+\frac{\eta_2}{\eta_1}c_1\dot{\varepsilon}+c_2(n_2+1)\varepsilon^{n_2}\dot{\varepsilon} \tag{9}$$

In summary, the one-dimensional constitutive relation given by Eq. (9) characterizes the observed viscoelastic behavior of typical polymeric materials under finite deformation. The functional expressions, η_1 and η_2, are dependent on strain rate and temperature; they decrease with increasing strain rate (shear thinning) and temperature (see Eq. (6)). Nonlinearity characteristics of the stress relaxation process is incorporated via a non-linear spring, this is represented by E_2. Moreover, the constitutive equation (9) represents a flexible framework for future generalizations to three-dimensional modeling.

Based on the differential equation (9), the stress drop during the room temperature relaxation is found out by substituting the strain rate equal to zero. The stress in this case can be written as:

$$\sigma=c_2\varepsilon_0^{(n_2+1)}+(\sigma_0-c_2\varepsilon_0^{(n_2+1)})\exp\left(-\frac{c_1t}{\eta_1}\right) \tag{10}$$

In this case the viscosity term given by Eq. (6) reduces to $(\eta(\dot{\varepsilon},T)=\eta_0)$ for experiments at reference temperature.

3.3. Effect of strain level

Fig. 7 presents the stress relaxation plot with the stress (σ MPa) against time of the studied elastomer at different strain levels of 100%, 200%, 320%, 400%, 500% and 600% at a constant strain rate of 30 mm/min. The data are indicating of significant physical relaxation involving rearranging of chains towards new configuration in equilibrium at the new strained state. The stress decay slows down with time as the system approaches equilibrium. The stress drops very quickly at first and then slows down appearing to approach a limit asymptotically at around 75% stress retention (approximately from 20% to 25% decay in stress) after large times at room temperature. This behavior is typical of most elastomers and is consistent with physical relaxation.

The stress relaxation data (Fig. 7) were used to calculate different material parameters involved in Eq. (10) such as c_1, c_2, n_2 and η. σ_0 is the initial stress level at which the relaxation begins. Also, ε_o represents the fixed strain at which the relaxation is performed. Using Eqs. (7) and (8), with the temperature term as unity at room temperature the linear and non-linear spring constants (E_1 and E_2) were found. Furthermore, the relaxation time of the dashpot can be calculated from the relation $\tau=\eta/E_2$ [13]. All these constants are presented in Table 3.

The model correlations obtained for the modified standard solid model along with the experimental data during relaxation are shown in Fig. 7. Note that the asymptotic behavior of the model presents a good correlation with the experimental data. The model captures even the transient part of the stress relaxation well. Although the results observed are quite close to observations still some scope for improvement is possible. In order to capture more accurately the relaxation response of the rubber matrix with the modified standard solid model, the addition of more relaxation times would be required. This could be accomplished by the addition of more Maxwell elements.

Fig. 8 shows the stress relaxation plot of the studied vulcanizates after immersion in kerosene for different time intervals of

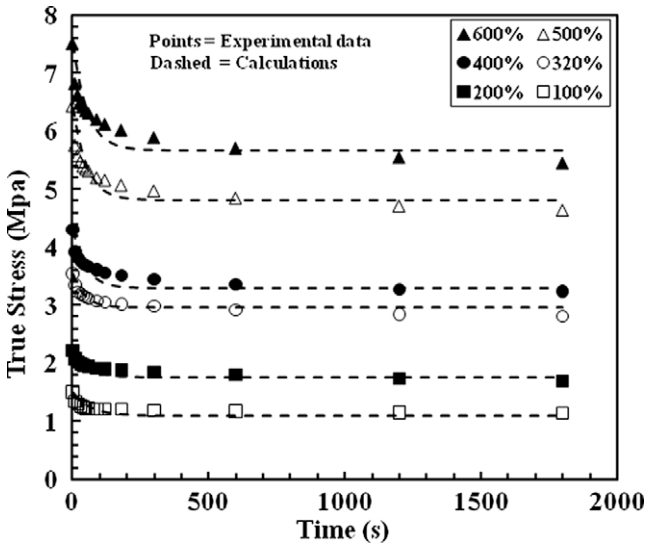

Fig. 7. Stress relaxation of 40HAF/NR at different strain levels and at a strain rate of 30 mm/min (points = experimental data, dashed lines = theoretic calculations).

10, 20, 40 min and 4 and 7 h at a strain level of 200% and at a constant strain rate of 30 mm/min. Attempts were made to make more investigations at higher swelling times and strain levels, but rapture of specimens limits the strain level and swelling times at the mentioned values. The same behavior of stress relaxation is detected as those in Fig. 5, but with changes in values and meanings of the material parameters which shown in Table 4. The values of the material parameters ($c_1 = E_1$, c_2, E_2, η and τ) are decreased with increasing the time of swelling as a result of chain cession caused by additional internal stresses generated by liquid molecules. This appears as a decrease in the relaxation time and also the value of the stress which needed to produce 200% strain at different swelling times shown in Fig. 9.

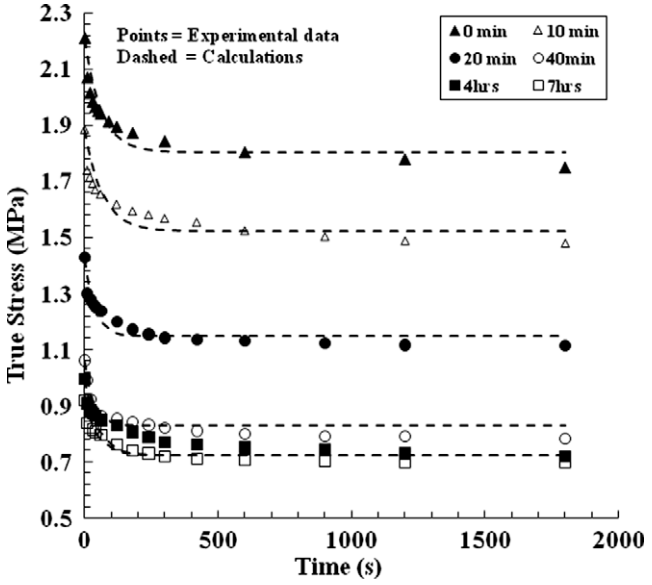

Fig. 8. Stress relaxation of 40HAF/NR at different swelling times, strain level of 200% and strain rate of 30 mm/min (points = experimental data, dashed lines = theoretic calculations).

Table 4
Material constants at different swelling time.

Time of swelling (min)	$c_1 = E_1$ (MPa)	c_2 (MPa)	n_2	$E_2 = c_2\varepsilon^n$ (MPa)	η (MPa s)	τ (min)
0	2.410	1.12	−0.35	0.89	1250	23.71
10	1.8	1.153	−0.6	0.76	1000	21.91
20	1.4	1	−0.8	0.57	800	23.21
40	1.2	0.8	−0.95	0.41	700	28.17
240	1.0	0.7	−0.96	0.36	500	23.16
420	1.0	0.7	−0.97	0.36	500	23.32

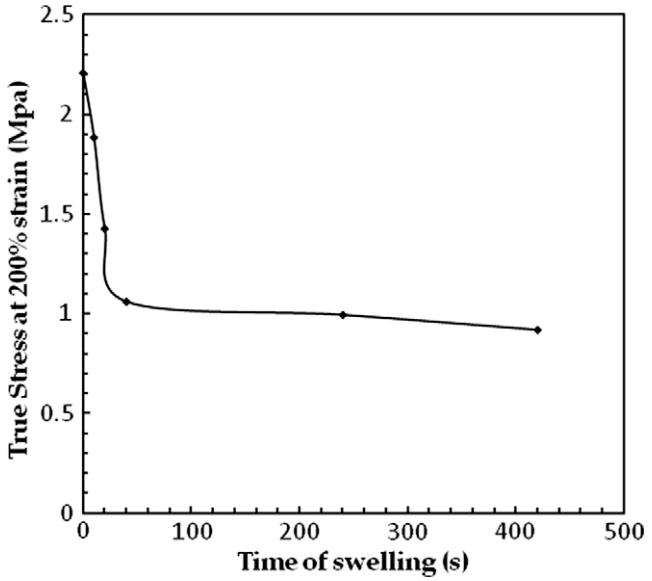

Fig. 9. Dependence of the true stress on swelling time for 40HAF/NR at a strain level of 200% and strain rate of 30 mm/min.

4. Conclusions

The uniaxial tensile stress relaxation behavior of natural rubber filled with carbon black is modeled using a modified standard solid model. The model is used to capture the response of NR matrix at different strain levels. A reasonably good agreement between the suggested model and the experimental data is found. Stress relaxation behavior is found to exhibit two step relaxation mechanism when straining the vulcanizate with high strain rates (greater than 30 mm/min). The behavior has one step relaxation mechanism at strain rate equal 30 mm/min.

Acknowledgment

The author would like to acknowledge College of Science as well as the dean ship of scientific research in King Faisal University for providing the facilities required for the present investigation.

References

[1] Attalla G, Guanela IB, Cohen RE. Effect of morphology on stress relaxation of polypropylene. Polym Eng Sci 1983;23:883–7.
[2] Andreassen E. Stress relaxation of polypropylene fibres with various morphologies. Polymer 1999;40:3909–18.
[3] Djokovic V, Kostaki D, Galovic S, Dramicanin MD, Kacarevic Z. Influence of orientation and irradiation on stress relaxation of linear low-density polyethylene (LLDPE): a two-process model. Polymer 1999;40:2631–7.
[4] Djokovic V, Kostaki D, Dramicanin MD, Suljovrujic E. Stress relaxation in high density polyethylene. Effects of orientation and gamma radiation. Polym J 1999;31:1194–9.
[5] Bhateja SK, Andrews EH. Effect of high energy radiation on the stress-relaxation of ultra-high molecular weight linear polyethylene. J Appl Polym Sci 1987;34:2809–17.
[6] Djokovic V, Kostoski D, Dramicanin MD. Viscoelastic behavior of semicrystalline polymers at elevated temperatures on the basis of a two-process model for stress relaxation. J Polym Sci B Polym Phys 2000;38:3239–45.
[7] Starkova O, Aniskevich A. Application of time–temperature superposition to energy limit of linear viscoelastic behavior. J Appl Polym Sci 2009;114:341–7.
[8] Sun J, Li H, Song Y, Zheng Q, He L, Yu J. Nonlinear stress relaxation of silica filled solution–polymerized styrene–butadiene rubber compounds. J Appl Polym Sci 2009;112:3569–74.
[9] Tager A. Physical Chemistry of Polymers. Moscow: Mir; 1987.
[10] Asaletha R, Bindu P, Aravind Indose, Meera AP, Valsaraj SV, Yang Weimin, et al. Stress-relaxation behavior of natural rubber/polystyrene and natural rubber/polystyrene/natural rubber–graft–polystyrene blends. J Appl Polym Sci 2008;108:904–13.
[11] Stevenson A, Campion RP. In: Gent AN, Editor. Engineering with rubber: how to design rubber components. Hanser: Munich; 1992.
[12] Geethamma VG, Pothen Laly A, Bhaskar Rhao, Neelakantan NR, Sabu Thomas. Tensile stress relaxation of short-coir-fiber-reinforced natural rubber composites. J Appl Polym Sci 2004;94:96–104.
[13] Patel M, Morrel PR, Murphy JJ. Continuous and intermittent stress relaxation studies on foamed polysiloxane rubber. Polym Degrad Stabil 2005;87:201–6.
[14] Madkour Tarek M. Step-strain stress relaxation of carbon black-loaded natural rubber vulcanizates. J Appl Polym Sci 2004;92:3387–93.
[15] Bhagawan SS, Triparthy DK, De SK. Stress relaxation in short jute fiber-reinforced nitrile rubber composites. J Appl Polym Sci 1987;33:1623–39.
[16] Flink P, Stenberg B. An indirect method which ranks the adhesion in natural rubber filled with different types of cellulose fibres by plots of $E(t)/E_t$ =0 versus log t. Brit Polym J 1990;22:193–9.
[17] Kutty SKN, Nando GB. Stress relaxation behavior of short Kevlar fiber-reinforced thermoplastic polyurethane. J Appl Polym Sci 1991;42:1835–44.
[18] Varghese S, Kuriakose S, Thomas S. Stress relaxation in short sisal-fiber-reinforced natural rubber composites. J Appl Polym Sci 1994;53:1051–60.

[19] Mackenzie CI, Scanlan J. Stress relaxation in carbon-black-filled rubber vulcanizates at moderate strains. Polymer 1984;25:559–68.
[20] Phillips JC. Stress relaxation of elongated strips of poly(vinylidene fluoride) in ethyl acetate vapor. Polym Eng Sci 1997;37:291–307.
[21] Nielson L. Mechanical Properties of Polymers and Composites, vol. 1. Marcel Dekker; 1987.
[22] Lockett FJ. Nonlinear viscoelastic solids. London: Academic Press; 1972.
[23] Christensen RM. Theory of viscoelasticity: an introduction. New York: Academic Press; 1982.
[24] Lubarda VA, Benson DJ, Meyers MA. Strain-rate effects in rheological models of inelastic response. Int J Plasticity 2003;19:1097–118.
[25] Khan AS, Suh YS, Kazmi R. Quasi-static and dynamic loading responses and constitutive modeling of titanium alloys. Int J Plasticity 2004;20:2233–48.
[26] Khan AS, Pamies OL, Kazmi R. Thermo-mechanical large deformation response and constitutive modeling of viscoelastic polymers over a wide range of strain rates and temperatures. Int J Plasticity 2006;22:581–601.